



**HAL**  
open science

# DECONFLICTING WIND-OPTIMAL AIRCRAFT TRAJECTORIES IN NORTH ATLANTIC OCEANIC AIRSPACE

Olga Rodionova, Daniel Delahaye, Banavar Sridhar, Hok K. Ng

► **To cite this version:**

Olga Rodionova, Daniel Delahaye, Banavar Sridhar, Hok K. Ng. DECONFLICTING WIND-OPTIMAL AIRCRAFT TRAJECTORIES IN NORTH ATLANTIC OCEANIC AIRSPACE. AEGATS '16, Advanced Aircraft Efficiency in a Global Air Transport System, AAF, Apr 2016, Paris, France. hal-01304633

**HAL Id: hal-01304633**

**<https://enac.hal.science/hal-01304633>**

Submitted on 20 Apr 2016

**HAL** is a multi-disciplinary open access archive for the deposit and dissemination of scientific research documents, whether they are published or not. The documents may come from teaching and research institutions in France or abroad, or from public or private research centers.

L'archive ouverte pluridisciplinaire **HAL**, est destinée au dépôt et à la diffusion de documents scientifiques de niveau recherche, publiés ou non, émanant des établissements d'enseignement et de recherche français ou étrangers, des laboratoires publics ou privés.

# DECONFLICTING WIND-OPTIMAL AIRCRAFT TRAJECTORIES IN NORTH ATLANTIC OCEANIC AIRSPACE

Olga Rodionova<sup>(1)</sup>, Daniel Delahaye<sup>(2)</sup>, Banavar Sridhar<sup>(3)</sup>, Hok K. Ng<sup>(4)</sup>

<sup>(1)</sup>Universities Space Research Association (USRA), NASA Ames Research Center, Moffett Field, Mountain View, CA, USA, [olga.p.rodionova@nasa.gov](mailto:olga.p.rodionova@nasa.gov)

<sup>(2)</sup>French Civil Aviation University (ENAC), 7 avenue Edouard Belin, Toulouse, France, [daniel@recherche.enac.fr](mailto:daniel@recherche.enac.fr)

<sup>(3)</sup>NASA Ames Research Center, Moffett Field, Mountain View, CA, USA, [banavar.sridhar@nasa.gov](mailto:banavar.sridhar@nasa.gov)

<sup>(4)</sup>University of California Santa Cruz, NASA Ames Research Center, Moffett Field, Mountain View, CA, USA, [hokkwan.ng@nasa.gov](mailto:hokkwan.ng@nasa.gov)

**KEYWORDS:** North Atlantic oceanic airspace, wind-optimal trajectories, conflict detection and resolution, deconflicting, aircraft trajectory optimization, Simulated Annealing, strategic flight planning.

## ABSTRACT:

North Atlantic oceanic airspace accommodates more than 1000 flights daily, and is subjected to very strong winds. Flying wind-optimal trajectories yields time and fuel savings for each individual flight. However, when taken together, these trajectories induce a large amount of potential en-route conflicts. This paper analyses the detected conflicts, figuring out conflict distribution in time and space. It further describes an optimization algorithm aimed at reducing the number of conflicts for a daily set of flights on strategic level. Several trajectory modification strategies are discussed, followed with simulation results. Finally, an algorithm improvement is presented aiming at better preserving the trajectory optimality.

## 1. INTRODUCTION

North Atlantic oceanic airspace (NAT) is the busiest oceanic airspace in the world that accommodates more than 1000 flights daily [1]. The flights crossing the NAT are subjected to very strong winds (Fig. 1) caused by the presence of the jet stream [2]. As a result, flight efficiency is greatly affected by these winds [3] and depends on the trajectory position in the wind field. Nowadays, aircraft rarely have the possibility to choose their optimal route, as they are restricted to follow predefined tracks called Organized Track System (OTS) [1]. However, with the upcoming development of new generation surveillance and broadcast technologies [4-6] leading to significant reduction in separation standards [7-10], flying flexible routes will become possible [11,12]. As a consequence, developing cost-optimal, and in particular, wind-optimal trajectories, is an important element of the aeronautical research.

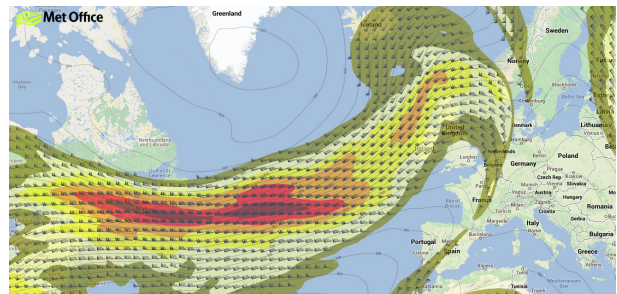


Figure 1. Example of jet stream wind field in NAT

A large amount of work is devoted to aircraft trajectory optimization in the presence of winds, for example, some of the most recent ones [12-16]. The results of these simulations demonstrate significant benefits that each particular aircraft could expect when flying wind- or climate-optimal route, including cruising time and fuel savings [17], and emissions and contrails reductions [18]. Nevertheless, when considered as a system, these sets of wind-optimal trajectories induce quite a large number of potential conflicts between flights [19], and the NAT becomes extremely congested. One reason for such a flight concentration is the nature of NAT flights: they mainly contribute to two opposite flows, eastbound and westbound, where the departure times for the flights in each flow are very close, because of passenger demands and time zone differences [1]. The other reason is the jet stream nature of wind fields: as a result the eastbound flights would try to follow the jet in order to benefit from strong tail winds, while the westbound flights would avoid the jet [15]. In order to enable safe flight progress, the airspace congestion should be reduced and the potential conflicts resolved.

Conflict detection and resolution is a complex problem that has been addressed in many different ways in literature [20]. The majority of studies are devoted to tactical conflict resolution (up to 30 minutes before a conflict occurs), where the most common maneuvers to avoid collisions are heading or speed changes [21-23]. Here,

deterministic optimization methods could be applied [24] as well as stochastic ones [25], where the optimization decision variables are authorized trajectory modification maneuvers. Algorithms devoted to strategic conflict resolution (performed before the aircraft take off) tend to be more computationally exhaustive, since they treat much greater number of aircraft at the same time [26]. All the works mentioned above address conflict resolution problem without considering winds.

The aim of the present research work is to combine the two important issues stated above, *i.e.* trajectory optimality in wind fields and conflict-free flight progress. We are interested in producing a wind-optimal conflict-free ensemble of aircraft trajectories for a given set of NAT flights on strategic level of trajectory planning (for a 24-hours time period). Several previous studies have already addressed such kind of a problem. In the approximate solution approach from [27], a wind-optimal trajectory for each aircraft is computed iteratively using aircraft dynamics in winds, and then it is modified in real time (by changing aircraft heading) in order to avoid all conflicts with the previously computed trajectories. In [28] all wind optimal trajectories are pre-computed beforehand, and the conflict resolution problem for these trajectories is formulated as a job-shop scheduling problem, with flight departure delays being the only optimization variables. In [29] first the congestion areas induced by pre-computed wind-optimal trajectories are identified, and then an iterative process based on Simulated Annealing is applied, where on each iteration step one of the trajectories is recalculated in order to avoid these congested areas. All the described methods have their limits of applicability.

In the present work, we develop an optimization method, based on strategic conflict resolution from [26], taking into account wind fields and trajectory optimality. Some preliminary results based on this method can be found in [19]. The paper is organized as follows. In Section 2, we describe our method of conflict detection and reveal some features on the nature of conflicts in NAT. In Section 3, the conflict resolution algorithm is presented, followed by the simulation results in Section 4. Finally, Section 5 describes how the algorithm can be extended in order to keep trajectories closer to wind-optimal ones. Section 6 summarized the main contributions of the paper.

## 2. CONFLICT DETECTION AND DISTRIBUTION

In order to develop an efficient conflict resolution method, it is useful to understand the nature and the structure of potential conflicts. This Section first describes the NAT flight data for wind-optimal trajectories that were used in our simulations. Then a conflict detection methodology is presented.

Finally, simulation results demonstrating conflict distribution in NAT are revealed.

### 2.1. Input data: wind-optimal trajectories in NAT

To perform the simulation of flight progress in NAT, we are given the wind field data, where  $u$  and  $v$  wind components are recorded with a defined step in a 3-dimension grid covering the world airspace. Each such grid corresponds to a particular hour of the day, with a 6-hours time step.

We perform our simulations for 31 days in July 2012. For each of these days, a set of wind-optimal trajectories is independently generated based on the equations of aircraft motion in wind [17]. For each aircraft, a resulting wind-optimal trajectory is given as a sequence of geographical points recorded each minute of flight starting from the departure airport and ending at the arrival airport. Thus, it can be considered as a sequence of 4D-points (latitude, longitude, altitude, time).

For simplification, each flight is supposed to cruise on a constant flight level at a constant speed. We are interested in cruising flight phase only, thus climbing and descending at origin and destination airports are not taken into account. Moreover, as our point of interest is NAT in particular, we focus on detecting conflicts in NAT only.

For each day, *i.e.* a 24-hours period, there are flights departing on this day, and arriving on the next day. Such flights should be taken into account when detecting conflicts not only for the current, but for the next day as well. For July 1<sup>st</sup> the total number of flights cruising on this day is incomplete, as we have no information about those flights departed on June 30<sup>th</sup>. Thus, we exclude the simulation results for July 1<sup>st</sup> from our statistics study, presented in the next sections.

### 2.2. Conflict detection methodology

By a classical definition, a conflict is a violation of established separation standards. Separation norms are typically defined for vertical, horizontal and, in some cases, temporal separation. In our case, vertical separation between aircraft on different flight levels, traditionally equal to 1000 feet, is maintained automatically. For horizontal separation, we apply a reduced separation norm, equal to 30NM. For comparison, a standard separation currently established in oceanic airspaces not covered by radar surveillance is 60NM. Moreover, nowadays aircraft crossing NAT within OTS are obliged to maintain temporal in-trail separation equal to 10 minutes. In our study, we also consider temporal separation, but reduced to 3 minutes. Note, that a commercial aircraft cruising at the highest speed in 3 minutes would cover a distance equal to about 30NM.

To detect conflicts according to the given separation standards, we apply point-to-point detection method based on the 4-dimensional grid from [26]. Such a grid is presented in Fig. 2, where the dimensions of the cells ( $\Delta_{lat}$ ,  $\Delta_{lon}$ ,  $\Delta_v$ ,  $\Delta_t$ ) are defined in correspondence with separation standards. Each 4D-trajectory point is placed in the appropriate cell depending on its coordinates, and then for each such point the separation between this point and all the points in the same and neighbor cells is verified. If for any point horizontal or temporal separation is violated, then a point-to-point conflict is detected. A pair of trajectories is in conflict, if any pair of their points is in conflict. Note, that ( $\Delta_{lat}$ ,  $\Delta_{lon}$ ,  $\Delta_v$ ,  $\Delta_t$ ) as well as the distance between the consecutive trajectory points should be chosen small enough in order not to miss potential conflicts occurring between points (see [30, 31] for more detail). In our case, we set  $\Delta_{lat}$  and  $\Delta_{lon}$  equal to 30NM,  $\Delta_v$  equal to 1000 feet, and  $\Delta_t$  equal to 15 seconds.

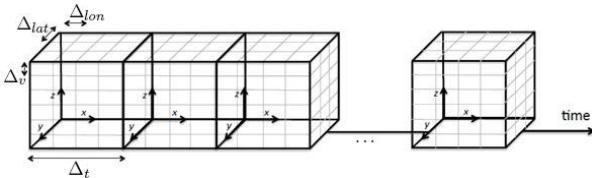


Figure 2. 4-dimensional grid for conflict detection

### 2.3. Initial number of conflicts

Using the methodology described above, we first focus on detecting the number of conflicts induced by initially generated wind-optimal trajectories. Below, the results of simulations for July 29<sup>th</sup> are presented. Conflict distribution for this day seems to be the worst among the 30 days, *i.e.* the most difficult for resolution. Fig. 3 demonstrates conflicts detected for a 24-hours time period on this day, where westbound trajectories are displayed in black, eastbound trajectories in blue, and conflict points in red (note, that only conflicts in NAT are taken into account). One can easily see that the opposite-direction flights mainly concentrate within two major flows, and conflicts have extremely high density within these flows.

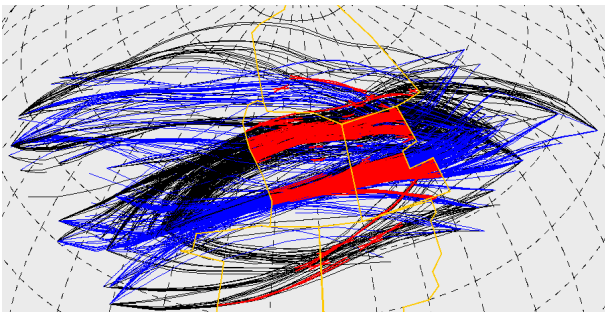


Figure 3. Initial conflict for wind-optimal trajectories

In Fig. 4, flight and conflict distribution over the 24 hours (with 30-minutes time step) is represented.

Here, when speaking about the number of conflicts, we mean the number of trajectory pairs involved in conflicts. As expected, conflict distribution reflects the flight distribution. Two peaks for the number of flights can be clearly distinguished. The first peak, around 0400 UTC (Coordinated Universal Time format, displaying GMT time, where first two digits stand for hours and last two digit stand for minutes), is related to the eastbound flow of flights departing North America in the evening. The second one around 1330 UTC is related to the westbound flow departing Europe in the morning. The peaks for the number of conflicts reflect the peaks for number of flights. While for July 29<sup>th</sup> the peak of conflicts corresponding to eastbound traffic is much more clearly distinguished, that is not always the case for other days.

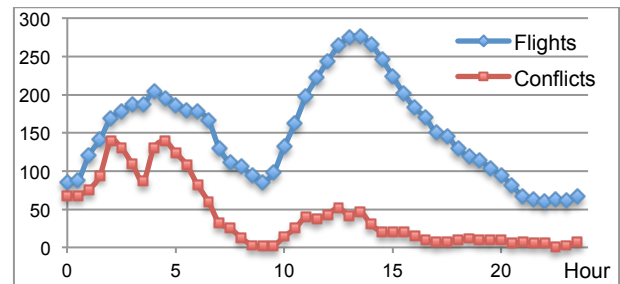


Figure 4. Flight and conflict distribution over 24 hours

Fig. 5 displays five Oceanic Control Areas (OCAs): Reykjavik, Shanwick, Gander, New York Oceanic and Santa Maria Oceanic, and Fig. 6 shows conflict distribution for these OCAs. As it can be seen, the majority of conflicts occur in Shanwick and Gander OCAs, while their number for other OCAs is almost negligible. From Fig. 6 it can be also seen how the peaks of conflicts migrate from Gander to Shanwick OCA between 0100 UTC and 0400 UTC, and then for eastbound traffic, and back from Shanwick OCA to Gander OCA between 1100 UTC and 1400 UTC for westbound traffic.

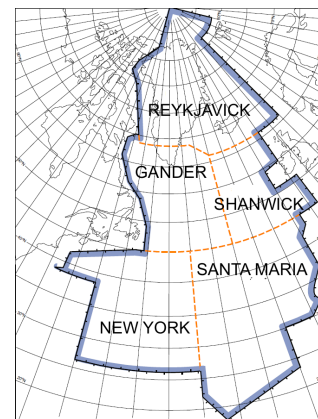


Figure 5. North Atlantic Oceanic Control Areas

These conflict distributions remain similar for other days being studied, while the number of conflicts

can largely vary from one day to another. Fig. 7 displays the number of flights and number of conflicts over 30 days in July 2012. The average number of daily flights is about 1130. The number of initially detected conflicts can be as large as 780 (for July 29<sup>th</sup>), with an average value being 533, and a minimal value being 349 (for July 23<sup>rd</sup>). The obtained results thus show, that the wind-optimal trajectories cannot be just flown as they are, and should be modified in order to avoid conflicts.

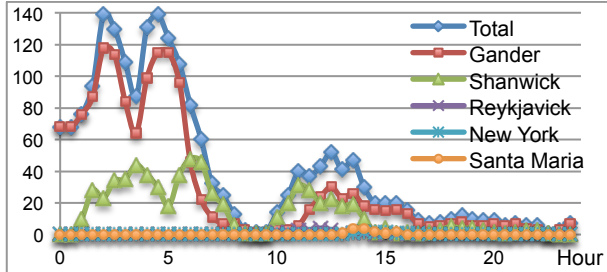


Figure 6. Conflict distribution over NAT OCAs

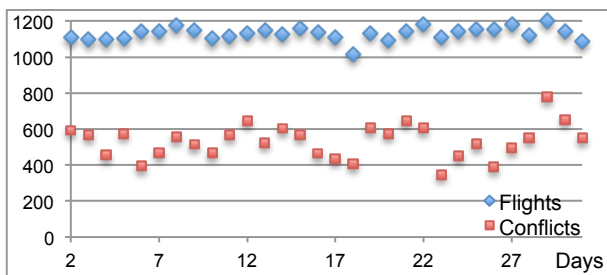


Figure 7. Number of flight and number of conflicts conflict over 30 days

## 2.4. Clusters of conflicts

In Section 2.3, the total number of conflicts for the daily sets of flights was investigated. Nevertheless, not all trajectories, marked in red in Fig. 3, are interacting with one another. Thus, an interesting point is to distinguish the conflict clusters, *i.e.* the subsets of trajectories, where each trajectory induce conflicts with at least one trajectory in the subset, and induce no conflict with any trajectory not belonging to the subset. Clusters identification could help to understand the nature and structure of the conflicts, and to propose more efficient strategies of conflict resolution.

Fig. 8 displays the total number of identified clusters for 30 days of July, as well as size of the maximal cluster, *i.e.* the maximal number of trajectories in a cluster. On average, there are about 150 different clusters daily. The majority of these clusters (about 73%) are of the size 2 or 3. Theoretically, conflict resolution inside such clusters should be easy. For each day, there are on average 6 clusters with the size equal or more than 10 (4% from the total cluster number), with maximal number of such clusters equal to 12. The number of trajectories in a maximal cluster is 25 on average, and reaches 56 in the worst case.

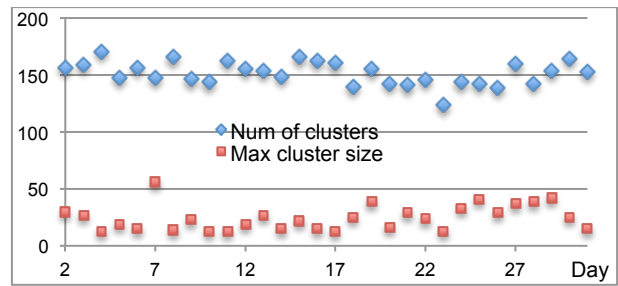


Figure 8. Number of clusters and number of trajectories in the largest cluster for 30 days

For July 29<sup>th</sup>, 154 different conflict clusters are identified, among which 104 are of the size 2 or 3. Eight clusters have the size more than 10, two of which are displayed in Fig. 9. The upper one involves 12 flights (conflict points displayed in magenta) from the westbound flight flow, avoiding jet. The lower cluster (conflict points shown in red) is the largest cluster for this day, consisting of 42 trajectories from the eastbound flow exploiting the jet wind. Conflict resolution for such a number of tightly interacting trajectories is much more complicated. However, not all of these conflicts occur at the same time moment.

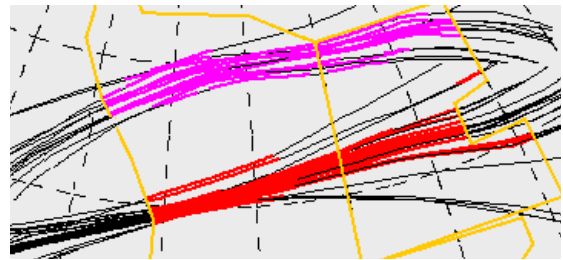


Figure 9. Two largest cluster of trajectories

Fig. 10 displays the distribution of the number of clusters and the largest cluster sizes over 24-hours time period for July 29<sup>th</sup>. This distribution reflects exactly the distribution of conflicts shown in Fig. 4. Note, that July 29<sup>th</sup> was found to be one of the worst days in terms of cluster formation. Fig. 11 demonstrates how the largest cluster propagates in time for a short time period from 0200 UTC to 0400 UTC. It is clearly seen how conflict positions move while the aircraft fly their eastbound routes.

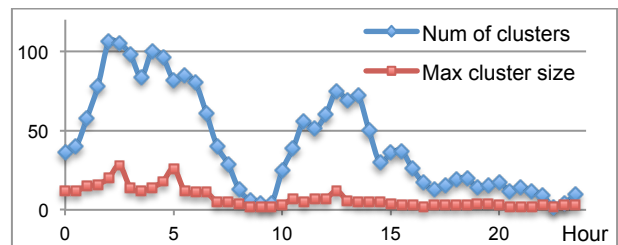


Figure 10. Number of clusters and number of trajectories in the largest cluster over 24 hours

From the conflict features we conclude that the highest congestion and the most difficult for conflict

resolution situations arise from clusters of trajectories that are very close to one another in space (parallel and/or identical) and time, and thus, are highly interrelated. Thus, one could think of a special method to resolve such types of conflicts. The efficient resolution in this case should be different from the resolution of a conflict between only two trajectories intersecting at a single point. Moreover, as shown in Fig. 11, the interactions inside a cluster tend to be time-dependent. Thus, a conflict resolution method could be time-dependent as well, performing consecutive resolution for a short time-period, and then shifting to the next time period. However, we keep these ideas as perspectives for future research. Section 3 describes the conflict resolution methodology applied in this study.

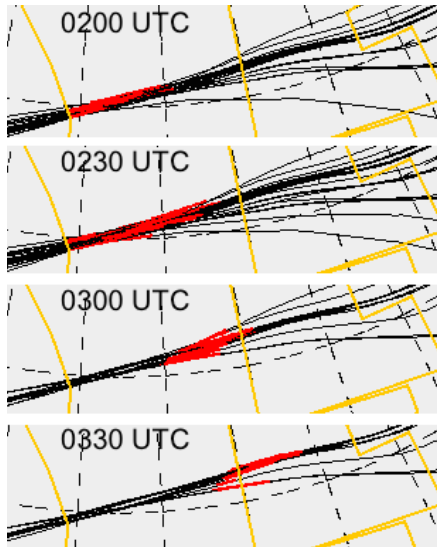


Figure 11. Largest cluster evaluation with time

### 3. CONFLICT RESOLUTION: METHODOLOGY

In order to resolve conflicts one need to modify initial wind-optimal trajectories. We would like to assure nevertheless that the resulting trajectories remain as close to the optimal ones as possible. In this Section we first describe the maneuvers applied for trajectory modification. Then we formulate a conflict resolution problem as an optimization problem with these maneuvers being the decision variable. Finally, we briefly describe the algorithm applied for the problem resolution.

#### 3.1. Trajectory modification maneuvers

In this study, we've selected two maneuvers to modify a given flight: to change its departure time and to change the geometrical shape of its trajectory. The procedure of departure time modification is very simple: it suffices to delay an aircraft  $f$  at each 4D-point of its trajectory by a given fixed time delay,  $d^f$ . The advantage of this method is that the trajectory optimality is not affected: strategic trajectory planning is made with

the assumption of constant wind fields. Too large delays are not desired by airlines, and the delays of several seconds have no sense in practice. Thus, we define  $d^f$  as a discrete variable taking integer values from 0 to 30 minutes maximum.

The procedure of trajectory shape modification is more complicated. We perform it in two steps: first we change the geographical position of the trajectory points (thus, the first two coordinates, latitude and longitude, of a 4D-point are modified), and next we recalculate the times when the aircraft passes these new points based on aircraft air speed (constant) and wind fields (i.e. the fourth coordinate, time, of a 4D-point is modified). To modify the geometrical shape of a trajectory, we exploit a bijective transformation between an arbitrary curve on a sphere and a curve on the  $xy$ -plane (Fig. 12).

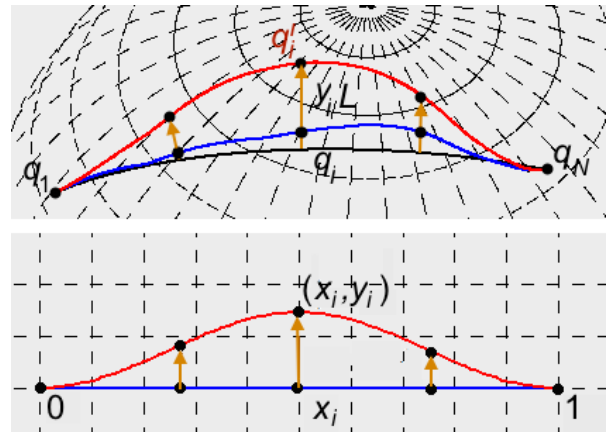


Figure 12. Trajectory shape modification approach

To do so, first we project each trajectory point on a spherical Earth,  $q_i$  (blue curve in Fig. 12) to a straight-line segment  $[0, 1]$  of  $x$ -axis, using the proportion of trajectory length up to this point to the total trajectory length,  $L$ , and obtain  $x_i$  values. Next, we modify the straight-line segment using a smooth function,  $y=\xi(x)$ , respecting boundary conditions, and obtain  $y_i$  values (bottom image in Fig. 12). Finally, we apply the bijection in another sense and shift each trajectory point  $q_i$  along a perpendicular to the great circle, joining the origin and destination point (black line in Fig. 12), on a distance proportional to  $y_i$  values and  $L$ , and obtain new points,  $q'_i$  (upper image in Fig. 12).

We decided to use a symmetric cosine-like function given by Eq. 1 that guarantees smooth trajectory modification:

$$\xi(x)=b^f Y(\cos(2\pi x-\pi)+1) \quad (1)$$

The function curvature can be controlled independently for each flight  $f$  using a single variable,  $b^f$ . We choose variables  $b^f$  to be real numbers from the segment  $[-1,1]$ . The actual trajectory deviation rate is then scaled by

multiplying these variables by a predefined maximal deviation value,  $Y$ . This value is set so that to assure that the maximal resulting curve length on  $xy$ -plane for any  $b^f$  does not exceed 1 by more than  $R_{max}$  percent, where  $R_{max}$  is a user-defined parameter.

### 3.2. Optimization problem formulation

We address the conflict resolution problem as an optimization problem. To do so, first we introduce the input data obtained from the given set of  $N$  wind-optimal trajectories. For each flight  $f$  from the set ( $f=1, \dots, N$ ) we have:

- $FL^f$  – aircraft flight level (constant);
- $v^f$  – aircraft speed (constant);
- $q^f=(\lambda_i^f, \varphi_i^f, a^f, t_i^f)$  – a sequence of 4D route points with coordinates (latitude, longitude, altitude, time).

Our decision variables originate from the authorized trajectory modification maneuvers, and are denoted for each flight  $f=1, \dots, N$  as described in Section 3.1:

- $d^f \in \{0, 1, \dots, N_{max}^d\}$  – departure time delay;
- $b^f \in [-1, 1]$  – a variable, controlling the rate of trajectory deviation from the initial one.

To simplify the exposition, we gather all the decision variables in a single vector,  $z$ :

- $z = (d^1, b^1, \dots, d^N, b^N)$ .

In the current formulation, the only constraints of the problem are the boundary constraints on the decision variables. The objective function is given by the total number of point-to-point conflicts induced by the set of modified trajectories corresponding to the variables  $z$ . We denote this function as  $C_t(z)$ . On doing so we obtain an optimization problem stated in Eq. 2:

$$\begin{aligned} \min_z C_t(z), \\ \text{s.t. } d^f \in \{0, 1, \dots, N_{max}^d\}, \\ b^f \in [-1, 1], f=1, \dots, N. \end{aligned} \quad (2)$$

The objective function,  $C_t(z)$ , cannot be explicitly represented in terms of decision variables,  $(d^f, b^f)$ . The value of this function for each instantiation of the decision variables is to be evaluated in the simulations (as described in Section 2.2). This problem is therefore a difficult high-dimensional mixed-integer black box (derivative-free) optimization problem. Thus, to resolve it we have chosen to use a stochastic algorithm.

### 3.3. Optimization algorithm

In the current work we implement a stochastic metaheuristic approach developed in [30] and extend it to the case of oceanic flights. This approach is based on the Simulated Annealing

algorithm. Simulated Annealing is a metaheuristic arising from the thermodynamics theory that imitates the annealing of the metal, involving heating and iterative process of controlled cooling. The classical Simulated Annealing scheme can be found in literature [32, 33]. Below one step of the iterative cooling process, implemented in our algorithm is described:

- Evaluate the current solution,  $z$ : calculate the number of induced conflicts,  $C_t(z)$ .
- Generate a neighbor solution  $z'$ :
  - Choose one flight,  $f$  (for example one of the most conflicted);
  - Randomly modify its trajectory (shape,  $b_f$ , or departure time,  $d_f$ );
  - Randomly modify all trajectories inducing conflicts with  $f$ .
- Reevaluate the new trajectory set,  $C_t(z')$ .
- Accept or reject this solution, with a probability  $p(z \rightarrow z', T)$  given by the Simulated Annealing scheme, where  $T$  is the current temperature during cooling process:

$$p(z \rightarrow z', T) = \begin{cases} 1, & \text{if } C_t(z') < C_t(z) \\ \exp\left(\frac{C_t(z) - C_t(z')}{T}\right), & \text{if } C_t(z') \geq C_t(z) \end{cases} \quad (3)$$

The iterative process stops when a conflict-free solution ( $C_t(z')=0$ ) is found, or when the maximal iteration number is achieved. The algorithm then yields the best solution, in terms of the number of aircraft pairs in conflict.

## 4. CONFLICT RESOLUTION: RESULTS

This section presents the results of conflict resolution. Several trajectory modification strategies were investigated:

- Modification of departure time only;
- Modification of trajectory shape only;
- Simultaneous modification of departure time and trajectory shape for NAT part of a trajectory;
- Simultaneous modification of departure time and trajectory shape for the complete trajectory from origin to destination.

Below, the comparison of the proposed strategies is presented.

### 4.1. Modification of trajectories within NAT

As our area of interest is NAT airspace, first we investigate the possibility to resolve conflicts by modifying trajectories within NAT only. The main criterion of the conflict resolution algorithm efficiency is the number of conflicts remaining after resolution. Fig. 13 displays the initial number of conflict for 30 days of July 2012, as well as the number of remaining conflicts after the resolution is accomplished. Here,  $T$  stands for departure time

modification, S stands for trajectory shape modification, and T+S stands for simultaneous time and shape modification. Fig. 14 displays the percent of reduced conflicts for each of the strategies.

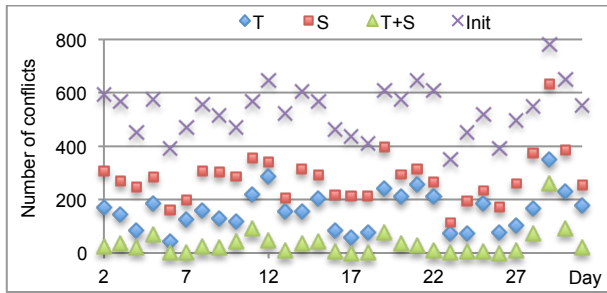


Figure 13. Number of initial conflicts and conflicts after resolution with different strategies

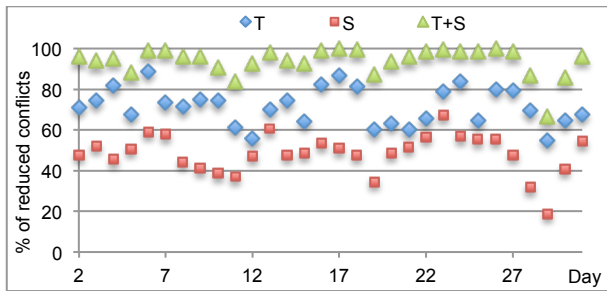


Figure 14. Percent of resolved conflicts for different strategies

As mentioned in Section 3.1, time modification only (T) is a good strategy, as it does not affect trajectory optimality. However, as can be seen from Fig. 12 and 13, it is not very efficient for conflict elimination. On average, only about 70% of the initial number of conflicts are resolved. Shape modification (S) gives even worthier results, with the average rate of conflict reduction equal to 50%. The best solution is yielded when time and shape modifications are applied in ensemble (T+S). For this strategy, there are two days, July 17<sup>th</sup> and 26<sup>th</sup> when all conflicts are completely eliminated. For all other days, except July 29<sup>th</sup>, less than 100 conflicts remain after resolution. On average, about 94% of initial conflicts are resolved for the 30 days, which is a very good result.

Figs. 15-17 visualize the remaining conflicts for July 29<sup>th</sup>, for each of the strategies, T, S and T+S respectively. Comparing to Fig. 3 their number is significantly reduced. However, as it can be seen from Fig. 15, modifying departure time is not sufficient for safely separating the aircraft in the major conflict clusters of eastbound flights (Figs. 9, 11): there are just much more aircraft in these clusters than can be allowed in the airspace with defined time-separation standards. In the same way, modifying only the shape within NAT is not sufficient neither, as trajectory points located near NAT boundaries (see Fig. 16) are not shifted enough to become separated. Combining both

strategists yields much better results. However, as shown in Fig. 17, the remaining conflicts are still located within the major conflict clusters and near NAT boundaries. Thus, we come to the conclusion that trajectory modification within NAT only is not very efficient.

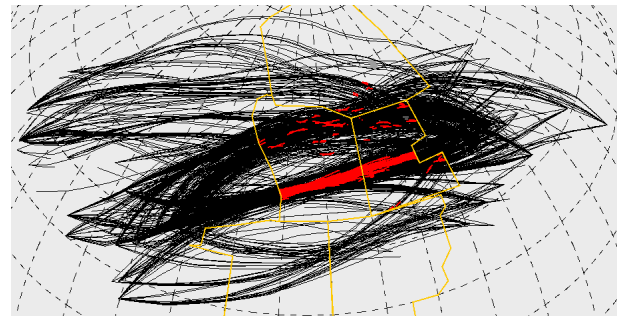


Figure 15. Remaining conflict when only time modification (T) is applied for resolution

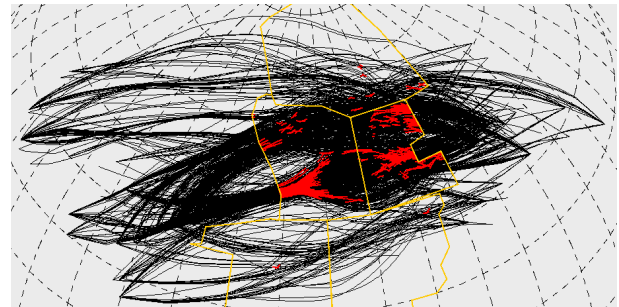


Figure 16. Remaining conflict when only shape modification (S) is applied for resolution

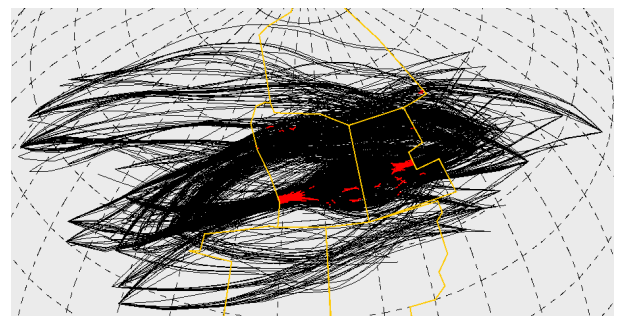


Figure 17. Remaining conflict with both time and shape modifications (T+S) applied for resolution

#### 4.2. Modification of complete trajectories

In the next step of our research we propose to modify the shape of a complete trajectory, from its origin to destination. We will refer to this strategy as T+Sc. The results are very encouraging: by adjusting the shape modification rate,  $R_{max}$  (a user-defined parameter, standing for the maximal allowed curve length increase in percent, see Section 3.1) we manage to eliminate all conflicts for all 30 days of July 2012. Fig. 18 shows the resulting trajectories for July 29<sup>th</sup> (simulations performed with  $R_{max}=2\%$ ). One can see that the traffic flows are much more large for these trajectories than for initial ones (Fig. 3).

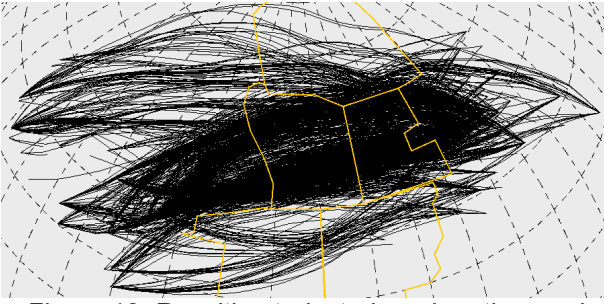


Figure 18. Resulting trajectories when time and shape modifications are applied to complete trajectories (T+Sc)

In order to obtain the best results, we investigate how the conflict resolution depends on trajectory shape modification rate,  $R_{max}$ . Tab. 1 presents some statistical results of simulations with different values of  $R_{max}$ . From Tab. 1 it can be seen, that the higher the modification rate is, the easier it is to resolve the conflicts: conflict-free solutions are obtained with higher probability, and faster. On the other hand, increase of the value of  $R_{max}$  leads to significant increase of the length for modified trajectories, and even more important increase of the cruising time for affected flights. Thus, the solutions obtained with high  $R_{max}$  are just not acceptable from an operational point of view. We assume that the most reasonable values for  $R_{max}$  are about 1-2%, which permit to resolve almost all conflicts and not to deviate trajectories too much.

Table 1. Comparison of conflict resolution results with different trajectory modification rates.

$R_{max}$ , %	0.5	1	2	3	5
Number of days with remaining conflicts	8	2	0	1	0
Average number of remaining conflicts per day	7	8	0	1	0
Average number of executed iterations when conflicts resolved	8.6	6.3	5.2	4.4	4.1
Average trajectory length increase, %	0.07	0.15	0.28	0.45	0.79
Average cruising time increase, %	0.32	0.55	0.96	1.33	1.99
Average number of modified trajectories	37.6	36.7	35.2	35.2	34.8
Maximal trajectory length increase, %	2.0	2.7	4.0	6.0	7.7
Maximal cruising time increase, %	4.6	5.9	14.1	10.3	16.1

Figs. 19-21 present the results of comparison of modification strategies T+S and T+Sc in terms of trajectory length and cruising time increase, and departure delays assigned (Fig. 21 includes T-strategy in comparison in addition). For T+S simulations,  $R_{max}=10\%$  was used (note, that this

modification rate is applied just for the NAT portion of a trajectory), while for T+Sc simulations, we selected  $R_{max}=2\%$ . T+Sc strategy definitively induces much less trajectory length increase. Time-increase deference for the two strategies is not as evident. However, T+Sc strategy tends to give better results for most of the days either. Moreover, it also yields less departure time delays. And that is in addition to total conflict elimination achieved by resolution with T+Sc. Thus, we come to the conclusion that the best resolution method involves complete trajectory modification combined with departure time modification.

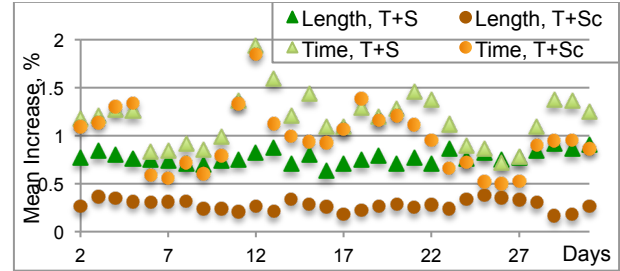


Figure 19. Average trajectory length and cruising time increase for two modification strategies

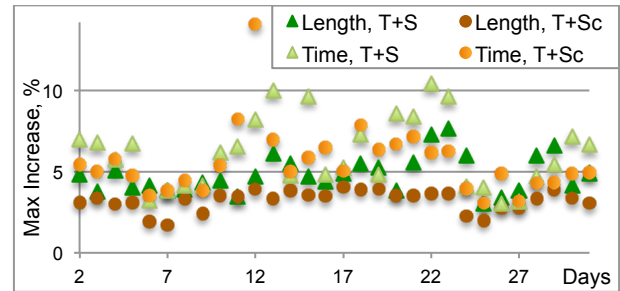


Figure 20. Maximal trajectory length and cruising time increase for two modification strategies

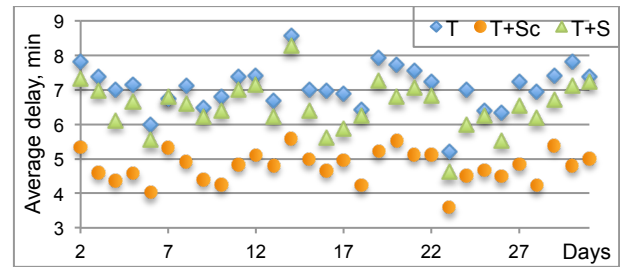


Figure 21. Average departure time delays for three modification strategies

## 5. TRAJECTORY OPTIMIZATION

In Section 4, we focused on conflict resolution only, and by modifying the departure time and trajectory shape, we managed to resolve all potential conflict for wind-optimal flights. However, on doing so, the flights are moved away from their desired routes. As a consequence, their cost increases. In this Section, we propose to extend the conflict resolution algorithm in order to make trajectory deviations as small as possible.

## 5.1. Optimization problem reformulation

In order to control trajectory deviations, we penalize these deviations, *i.e.* departure time and trajectory shape modifications, and include these penalties into the objective function from Eq. 2 with adjusted weighting coefficients. Thus, in addition to the total number of conflicts,  $C_t(z)$ , for each instantiation of decision variables,  $z$ , we compute the following values:

- $\Delta T_c(z)$  – total cruising time increase evaluated over  $N$  trajectories; and
- $\Delta T_d(z)$  – total departure time delays assigned to  $N$  trajectories.

The resulting objective function is given by Eq. 4:

$$\min_z C_t(z) + \alpha \Delta T_c(z) + \beta \Delta T_d(z), \quad (4)$$

where  $\alpha$  and  $\beta$  are user-defined weighting coefficients that permit to control the trade-offs between the values being optimized.

## 5.2. Simulation results

Below we perform the results for two test cases, and we compare these results with simple conflict resolution described in Section 4.2. In the first case, further referred as T+Sc+C, we would like to minimize cruising time increase only, and thus, we set coefficient  $\beta$  equal to 0. In the second case, referred as T+Sc+C+D, we consider both cruising time increase, and departure delay, with  $\alpha=1/600$ , and  $\beta=0.2\alpha$ . Figs. 22-26 demonstrate the results of comparison.

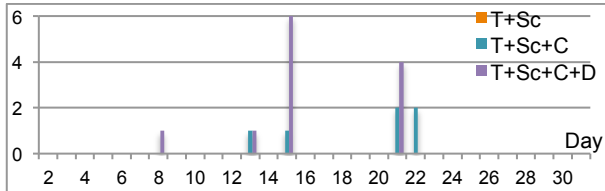


Figure 22. Number of remaining conflicts for three optimization strategies

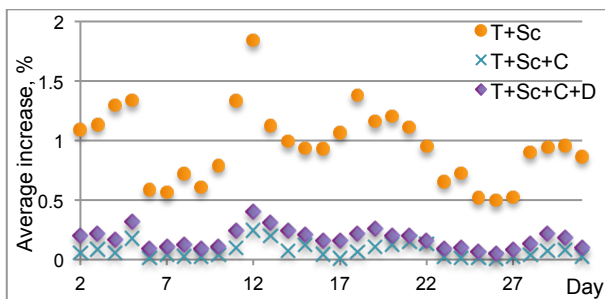


Figure 23. Average cruising time increase for three optimization strategies

First, one can notice, that when trajectory deviations are taken into account, there appear several days, for which not all conflicts are eliminated (Fig. 22), even if the number of remaining conflicts is really small. However, we

recall that we are performing strategic conflict resolution, and thus, any remaining conflict could be further resolved during tactical phase. Moreover, in reality flights would never fly exactly the given routes, because of different hazardous conditions, including changing meteorological conditions. Thus, the predicted conflicts might never happen in the reality, while new conflicts could reappear. Thus, our goal is not to eliminate completely all the conflicts, but to separate the trajectories sufficiently in order to reduce the airspace congestion in general. Note in addition, that even the actual flight routes issued to the real flights in the strategic planning phase when evaluated as an ensemble induce quite a large number of conflicts. These conflicts however would never happen in the reality and are typically addressed in the tactical phase.

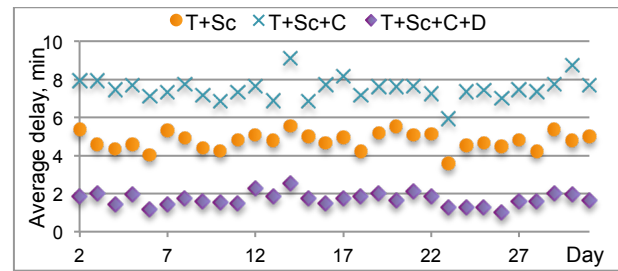


Figure 24. Average departure time delay for three optimization strategies

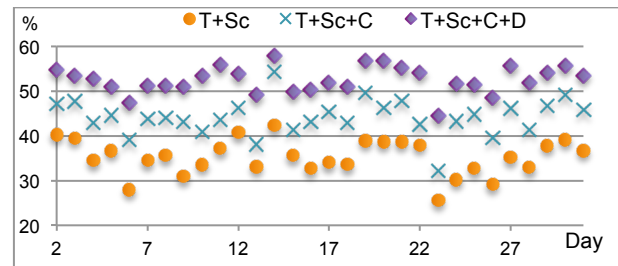


Figure 25. Average percent of flights with modified trajectories for three optimization strategies

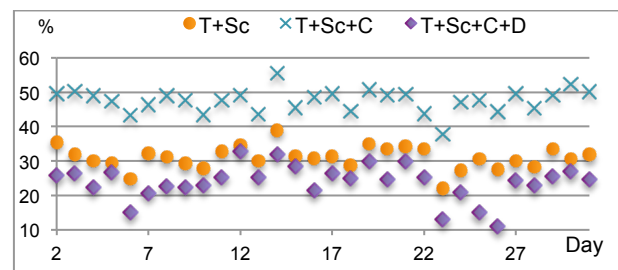


Figure 26. Average percent of delayed flights for three optimization strategies

On the other hand, one can see from Fig. 23, that when penalties on trajectory shape modification are included in the optimization (blue crosses), the average cruising time increase is significantly smaller than when these modifications are ignored (orange circles). This is a major argument to use such an extended conflict resolution algorithm.

When penalties on departure delays are in addition included in the optimization (T+Sc+C+D case), these departure delays are significantly decreased, by more than two comparing to T+Sc strategy, and by about 3 comparing to T+Sc+C strategy (Fig. 24). At the same time, the cruising time (violet diamonds in Fig. 23) is not increased a lot comparing to the results of T+Sc+C simulation (blue crosses). Thus, considering both deviation maneuvers seems to be the most reasonable way to tackle the exposed problem.

## 6. CONCLUSION

The current paper presents a comprehensive study on the nature and the structure of conflict induced by a set of wind-optimal trajectories in North Atlantic oceanic airspace. We discovered how conflicts are distributed in space and time, and we revealed that the most difficult conflict resolution situations are due to intensive conflict clusterization within the main traffic flows.

We then addressed conflict resolution problem in order to reduce the congestion in NAT. We formulated this problem as an optimization problem, introduced acceptable ways of wind-optimal trajectories modification, and developed a stochastic optimization algorithm, capable to manage different strategies of conflict resolution. Moreover, an extended version of the algorithm permits not only to reduce the number of conflicts, but also to keep the resulting trajectories as close to wind-optimal ones as possible.

We recall that our goal was general conflict reduction and not complete conflict elimination, as the simulations were performed for the strategic trajectory planning that is done such in advance, that the conditions used in the simulations (in particular, the winds) would differ from actual conditions experienced by aircraft en-route. As a result, new conflicts may reappear in the issued conflict-free trajectories. These conflicts then are to be addressed during tactical conflict resolution. That is what currently happening in the reality, as even the actual routes issued to aircraft induce quite a large number of conflicts.

From the obtained results, we conclude, that the best way to reduce the number of conflicts is to simultaneously modify departure time and geometrical shape of the trajectories, while applying these maneuvers separately does not allow sufficient flexibility to avoid all the conflicts. Furthermore, considering trajectory modifications while performing conflict resolution permits to significantly reduce these modifications without affecting the efficiency of the resolution greatly.

One of the possible ways to extend the presented work is to look deeply into conflict clusters structure and try to elaborate different resolution

strategies for different cluster types, involving Data Mining tools. This method could give smarter trajectory modifications and more acceptable solutions.

Another idea is to distribute conflict resolution in time, by resolving conflicts just inside short-period overlapping time windows consecutively. In this case, the resolution on each step will involve smaller number of trajectories and thus, should be simpler. In addition to this, trajectories would be perturbed for smaller portions of their length.

Finally, we could address the main drawback of strategic trajectory planning, *i.e.* its robustness regarding changing flight conditions, in particular, meteorological conditions. Taking into account uncertainties in wind prediction while performing conflict resolution could increase significantly the robustness of the yielded solutions, and that is a good challenge for future work.

## 7. ACKNOWLEDGEMENTS

This research was supported by an appointment to the NASA Postdoctoral Program at NASA Ames Research Center, administrated by Universities Space Research Association through a contract with NASA.

## 8. REFERENCES

1. NAT Doc 007, *Guidance concerning air navigation in and above the North Atlantic MNPS airspace* (2012). International Civil Aviation Organization (ICAO).
2. Woollings, T., Hannachi, A. & Hoskins, B. (2010). Variability of the North Atlantic eddy-driven jet stream. *Quarterly Journal of the Royal Meteorological Society*, **136**, pp856–868.
3. Office of Aviation Enforcement and Aviation Consumer Protection Division Proceedings. (2015). Air Travel Consumer Report, U.S. Department of Transportation.
4. Nolan, M.S. *Fundamentals of Air Traffic Control* (2010). Cengage Learning.
5. Couluris, G.J. (1990). Automatic dependent surveillance benefit and cost analysis. Technical report, U.S. Department of Transportation, Federal Aviation Administration.
6. Draft Implementation Plan for the Trial Application of RLatSM in the NAT Region (2013). Technical report, European and North Atlantic (EUR/NAT) Office.
7. Gerhardt-Falk, C.M., Elsayed, E.A. Livingston, D. & Colamosca, B. (2000). Simulation of the North Atlantic Air Traffic and

- Separation Scenarios. Technical report, U.S. Department of Transportation, Federal Aviation Administration.
8. Williams, A. & Greenfeld, I. (2006). Benefits Assessment of Reduced Separations in North Atlantic Organized Track System. 6th AIAA Aviation, Technology, Integration, and Operations Conference (ATIO).
  9. Louyot, P. (2007). ASEP-ITM simulations from traffic data. Technical report, Advanced Safe Separation Technologies and Algorithms (ASSTAR) Project.
  10. Rodionova, O., Sbihi, M., Delahaye, D. & Mongeau, M. (2014). North Atlantic Aircraft Trajectory Optimization. *IEEE Transactions on Intelligent Transportation Systems*, **15**(5), pp2202–2212.
  11. Viets, K.J. & Ball, C.G. (2001). Validating of Future Operational Concept for En Route Air Traffic Control. *IEEE Transactions on Intelligent Transportation Systems*, **2**(2), pp63–71.
  12. Kirk, D.B., Heagy, S.H. & Yablonski, M.J. (2001). Problem Resolution Support for Free Flight Operations. *IEEE Transactions on Intelligent Transportation Systems*, **2**(2), pp72–80.
  13. Andresson, E.I. (2012). Lateral Optimization of Aircraft Tracks in Reykjavik Air Traffic Control Area. PhD thesis, School of Science and Engineering, Reykjavik University.
  14. Wickramasinghe, N.K., Harada, A. & Miyazawa, Y. (2012). Flight Trajectory Optimization for an Efficient Air Transportation System. 28th International Congress of the Aeronautical Science (ICAS 2012).
  15. Irvine, E.A., Hoskins, B.J., Shine, K.P., Lunnon, R.W. & Froemming, C. (2013). Characterizing North Atlantic weather patterns for climate-optimal aircraft routing. *Meteorological Applications*, **20**, pp80–93.
  16. Girardet, B., Lapasset, L., Delahaye, D. & Rabut, C. (2014). Wind-optimal path planning: Application to aircraft trajectories. 13th International Conference on Control, Automation, Robotics and Vision.
  17. Sridhar, B., Ng, H.K., Linke, F. & Chen, N.Y. (2014). Benefits Analysis of Wind-Optimal Operations For Trans-Atlantic Flights. 14th AIAA Aviation Technology, Integration, and Operations Conference.
  18. Ng, H.K., Sridhar, B., Chen, N.Y. & Li, J. (2014). Three-Dimensional Trajectory Design for Reducing Climate Impact of Trans-Atlantic Flights. 14th AIAA Aviation Technology, Integration, and Operations Conference.
  19. Sridhar, B., Chen, N.Y., Ng, H.K., Rodionova, O., Delahaye, D. & Linke, F. (2015). Strategic Planning of Efficient Oceanic Flights. Eleventh USA/Europe Air Traffic Management Research and Development Seminar (ATM2015).
  20. Kuchar, J.K. & Yang, L.C. (2000). A Review of Conflict Detection and Resolution Modeling Methods. *IEEE Transactions on Intelligent Transportation Systems*, **1**(4), pp179–189.
  21. Mao, Z.H., Feron, E. & Bilimoria, K. (2001). Stability and Performance of Intersecting Aircraft Flows Under Decentralized Conflict Avoidance Rules. *IEEE Transactions on Intelligent Transportation Systems*, **2**(2), pp101–109.
  22. Pallottino, L., Feron, E., & Bucchi, A. (2002). Conflict Resolution Problem for Air Traffic Management Systems Solved with Mixed Integer Programming. *IEEE Transactions on Intelligent Transportation Systems*, **3**(1), pp3–11.
  23. Christodoulou, M.A. & Kodaxakis, S.G. (2006). Automatic Commercial Aircraft-Collision Avoidance in Free Flight: The Three-Dimensional Problem. *IEEE Transactions on Intelligent Transportation Systems*, **7**(2), pp242–249.
  24. Dougui, N., Delahaye, D., Peuchmorel, S. & Mongeau, M. (2013). A light propagation model for aircraft trajectory planning. *Journal of Global Optimization*, **56**(3), pp873–895.
  25. Delahaye, D., Peyronne, C., Mongeau, M. & Peuchmorel, S. (2011). Aircraft conflict resolution by genetic algorithm and B-spline approximation. 2nd ENRI International Workshop on ATM/CNS, pp71–78.
  26. Chaimatanan, S., Delahaye, D. & Mongeau, M. (2014). A Hybrid Metaheuristic Optimization Algorithm for Strategic Planning of 4D Aircraft Trajectories at the Continental Scale. *IEEE Computational Intelligence Magazine*, **9**(4), pp46–61.
  27. Jardin, M.R. (2003). Real-time conflict-free trajectory optimization. 5th USA/Europe Air Traffic Management Research and Development Seminar (ATM 2003 R&D).
  28. Grabbe, S., Sridhar, B. & Mukherjee, A. (2008). Scheduling Wind-Optimal Central East Pacific Flights. *Air Traffic Control Quarterly*, **16**(3), pp187–210.
  29. Girardet, B. (2014) Trafic aerien: determination optimale et globale des

trajectoires d'avion en presence de vent. PhD thesis, General Mathematics, Toulouse INSA.

30. Chaimatanan, S. (2014). Strategic aircraft trajectory planning. PhD thesis, Toulouse University III Paul Sabatier.
31. Rodionova, O. (2015). Aircraft trajectory optimization in North Atlantic oceanic

airspace. PhD thesis, Toulouse University III Paul Sabatier.

32. Kirkpatrick, S., Gelatt, C.D. & Vecchi, M.P.G. (1983). Optimization by Simulated Annealing. *Science*, 220, pp671–680.
33. Aarts, E. & Korst, J. (1989). *Simulated Annealing and Boltzmann Machine*. John Wiley and Sons.